Semicond. Sci. Technol. **22** (2007) 1189–1192 doi:10.1088/0268-1242/22/11/001

Exciton–photon coupling in a ZnSe-based microcavity fabricated using epitaxial liftoff

A Curran, J K Morrod, K A Prior, A K Kar and R J Warburton

School of Engineering and Physical Sciences, Heriot-Watt University, Edinburgh EH14 4AS, UK

E-mail: a.curran@hw.ac.uk

Received 28 May 2007, in final form 20 August 2007
Published 2 October 2007
Online at stacks.iop.org/SST/22/1189

Abstract

We report the observation of strong exciton–photon coupling in a ZnSe-based microcavity fabricated using epitaxial liftoff. Molecular beam epitaxial grown $ZnSe/Zn_{0.9}Cd_{0.1}Se$ quantum wells with a one wavelength optical length at the exciton emission were transferred to a SiO_2/Ta_2O_5 mirror with a reflectance of 96% to form finesse matched microcavities. Analysis of our angle-resolved transmission spectra reveals key features of the strong coupling regime: anticrossing with a normal mode splitting of 23.6 meV at 20 K, composite evolution of the lower and upper polaritons and narrowing of the lower polariton linewidth near resonance. The heavy-hole exciton oscillator strength per quantum well is also deduced to be 1.78×10^{13} cm^{-2}.

(Some figures in this article are in colour only in the electronic version)

1. Introduction

Light–matter interaction inside quantum microcavities (MCs) containing one or more quantum wells (QWs) has seen growing interest since the first experimental observation of the normal mode splitting of the coupled oscillators [1]. The two coupled states, the lower and upper cavity polaritons, are the result of the strong hybridization of the resonant cavity photon and QW exciton. The cavity polariton lends itself to the possibility of a thresholdless laser [2–4], ultrafast micro-optical amplifiers [5, 6] and Bose–Einstein condensation (BEC) in a solid state environment [7].

Much of the work done in this area has focused on III–V MCs [1, 5, 6, 8] because of the high quality QWs and GaAs/AlAs distributed Bragg reflectors. However, the low binding energy of excitons found in typical III–V QWs (5–10 meV) is not ideal. Saba *et al* [6] show that the cut-off temperature for polariton parametric scattering, the proposed mechanism for a thresholdless laser, is determined by the exciton binding energy, and therefore room temperature operation is prohibited for GaAs QWs. Achieving BEC in MCs also requires sufficiently large binding energies such that the critical density can be reached before ionization. Wide bandgap II–VI-based MCs are a promising alternative since the typical binding energy (∼30 meV) is comparable to the room temperature thermal energy [9]. However, fabrication of II–VI MCs is a challenge with all growth techniques since suitable materials that satisfy the lattice matching criteria are in their infancy. To the best of our knowledge there are only a few demonstrations of II–VI-based MCs, either involving growth-etch-growth processing [10, 11] or the use of semiconductor mirrors [3, 7, 13]. Hybrid devices are challenging to fabricate in our experience because of the difficulties in controlling the etching at the interface between the GaAs substrate and the ZnSe epilayer. II–VI semiconductor mirrors require complex layer sequences to mimic alloy compounds and to avoid the build-up of strain. Large light penetration depth due to the low refractive index contrast is an inherent disadvantage of the monolithic approach. To date, a hybrid device has shown exciton photon coupling in a ZnCdSe/ZnSe heterostructure [10, 11] and the Purcell effect for a CdSe/ZnSe quantum dot [14]. Monolithic devices have shown clear strong coupling for CdTe [3, 7] and GaN [12] QWs, but not for ZnSe QWs.

We report here the successful fabrication and characterization of ZnSe-based MCs using a new hybrid technology. We use a selective etching technique, epitaxial

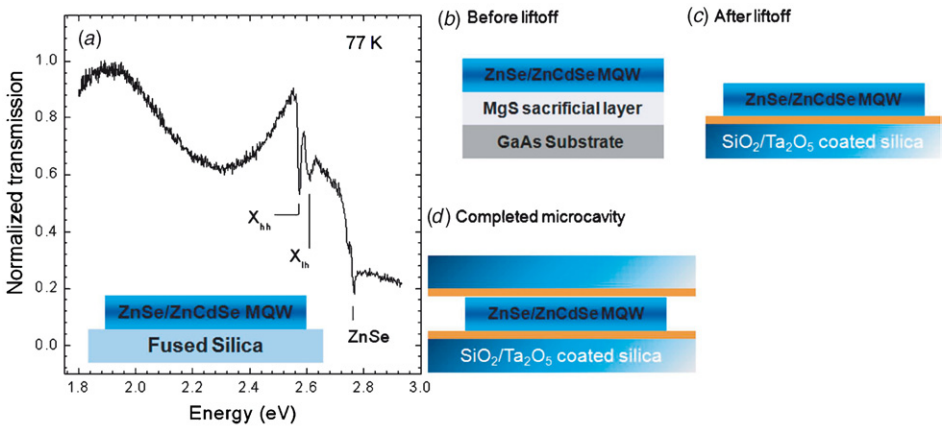

Figure 1. (*a*) Normalized transmission of the ZnSe/$Zn_{0.9}Cd_{0.1}$Se QWs used as the active medium of the MC. Reference samples were lifted and transferred to a fused silica substrate. Inset: schematic of the QWs transferred to a glass substrate. (*b*)–(*d*) Schematics of the sample at each stage of the MC fabrication (not to scale).

liftoff [15], to transfer the ZnSe epilayer to a high quality dielectric mirror. This new technology has allowed us to fabricate high quality ZnSe-based MCs without the problems encountered with previous hybrid technologies. Also, the dielectric mirrors have short penetration lengths, conferring stronger exciton–photon coupling than can be achieved with monolithic MCs. The large binding energies found in ZnSe-based QWs combined with the high performance of dielectric mirrors make our samples ideally suited to the study of parametric scattering and BEC.

2. Sample fabrication

The active region of the cavity was grown by molecular beam epitaxy on high quality GaAs n^+-substrates following the deposition of a 20 nm ZnSe buffer layer. A sacrificial layer of MgS (10 nm) was grown [16], then the active region, 5 ZnSe (8 nm)/$Zn_{0.9}Cd_{0.1}$Se (8 nm) QWs with ZnSe spacers' (∼53 nm) top and bottom such that the thickness of the active layer was equal to one optical wavelength at the emission of the well. Rotation of the sample was stopped during the growth of the top ZnSe spacer so as to allow translational tuning of ∼10 meV mm^{-1} of the completed MC. Small 3×3 mm^2 samples from the wafer were prepared by cleaving and coated with wax. The MgS sacrificial layer was selectively etched in a solution of HCl acid to free the active layer from the GaAs substrate. The lifted layer, supported by the layer of wax, was then transferred to a SiO_2/Ta_2O_5 dielectric mirror. Details of the liftoff technique are reported elsewhere [15]. Our mirrors are specifically designed such that the cavity linewidth, γ_{cav}, and electric field profile were optimum for strong coupling with our quantum wells[1]. This involves matching the cavity linewidth to the exciton linewidth (9.2 meV at 20 K) and positioning the QWs at the antinode of the electric field distribution. The mirror transmission was measured to be 3.9% at 475 nm with a structure designated by $g(LH)^7La$ (L: SiO_2, $n = 1.46$; H: Ta_2O_5, $n = 2.1$; and a: air, $n = 1.0$). Finally, a second dielectric mirror was mechanically held against the active layer forming a MC of cavity length $L_{cav} \sim 170$ nm [2] and refractive index $n_{cav} = 2.78$. The resultant Q of the cavity is modest, ∼200, limited by the relatively low reflectivity of the mirrors. We expect an increase in the mirror reflectivity to result in a much higher Q. The completed MCs were transferred to a continuous flow cryostat and characterized at 20 K. All our fabrication steps were carried out in an air-filtered environment, reducing the possibility of dust particles becoming trapped within the MC.

Reference samples were lifted and transferred to fused silica substrates and characterized by measuring their transmission at 77 K. White-light continuum generated with fs pulses from a Ti:sapphire laser was focused to a spot size of 20 μm on the sample. The sample was normal to the optical axis. The transmitted light was collected with an angular resolution of 0.2° at normal incidence by a 500 μm multi-mode fibre bundle. The collected light was dispersed with a spectrometer with a resolution of 0.1 nm and imaged onto a liquid nitrogen cooled CCD camera. Figure 1 shows the transmission of five ZnSe/$Zn_{0.9}Cd_{0.1}$Se QWs lifted and transferred to a fused silica substrate. Two main optical features are the heavy-hole exciton $X_{hh} = 2.575$ eV and light-hole exciton $X_{lh} = 2.611$ eV transitions. A low energy oscillation is clear and is attributed to interference within the overall epitaxial layer. High energy features around 2.77 eV correspond to bulk transitions in the ZnSe barriers. This experiment demonstrates that the liftoff step preserves the high optical quality of the ZnCdSe/ZnSe QWs.

3. Results

The definitive experiment when searching for cavity polaritons is the measurement of the optical angular dispersion. In the weak coupling regime, the two states disperse independently. In the strong coupling regime the observed dispersion curves are distinctly altered on and near resonance, where they

[1] The bare exciton linewidth, $\gamma_{X_{hh}} = 9.2$ meV, was matched to $\gamma_{cav} \sim 15$ meV, satisfying $\Omega^2 \gg (\gamma_{X_{hh}} - \gamma_{cav})^2$. The stacking order of the $\frac{\lambda}{4}$ layers was such that the antinode of the electric field inside the cavity was positioned at the quantum wells.

[2] The epitaxial layer thickness deduced from figure 1 was used in the coupled oscillator model in figure 3(*b*).

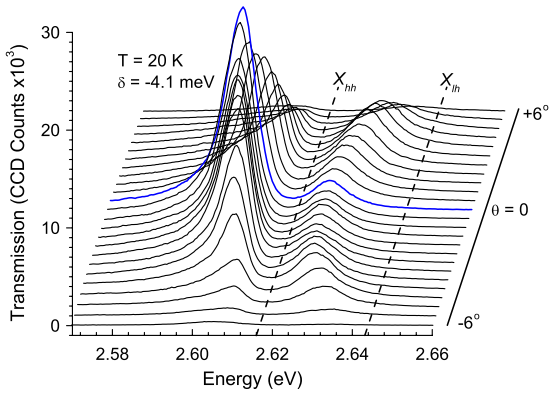

Figure 2. Angle-resolved transmission spectra taken at spatial points in the first Fourier plane of the collection lens. The sample was detuned by -4.1 meV at $\theta = 0^\circ$ and scanned through $\pm 6^\circ$. The dashed lines mark the uncoupled heavy-hole, $X_{\rm hh}$, and light-hole, $X_{\rm lh}$, exciton transitions. The normal incidence spectrum is highlighted. Spectra are offset for clarity.

anticross with a normal mode splitting (Rabi splitting), typically a few meV.

Completed microcavities were characterized by measuring white light transmission at 20 K. Two identical lenses, NA matched to the cryostat, were used to focus and collect light at the sample. Fully illuminating the objective lens, white light was focused at the sample and the transmitted light was collimated to a diameter of 33 mm, where a fibred coupled spectrometer was used to scan through the collimated light and thus record a series of transmission spectra. In this way lateral displacement is related to angular dispersion inside the MC. Taking into account the glass substrate of the mirrors, the range of angle at the MC surface was $\pm 6^\circ$. Each spectrum was taken at different points through the centre of the collimated beam with increments of 1 mm. Since the in-plane wavevector inside the cavity, $k_\parallel$, is related to the angle of incident light by $k_\parallel = \frac{\omega_{\rm cav}}{c}\sin(\theta)$, we can measure the dispersion curves of our samples in k-space between $\pm 1.39 \times 10^6$ m^{-1}. Figure 2 shows a series of spectra taken for one of our samples detuned to $\delta = -4.1$ meV relative to the $X_{\rm hh}$ transition at normal incidence. The spectra are offset with the lowest spectrum corresponding to $k_\parallel = -1.39 \times 10^6$ m^{-1} (-6°), increasing to $k_\parallel = 1.39 \times 10^6$ m^{-1} ($+6^\circ$). The uncoupled $X_{\rm hh}$ and $X_{\rm lh}$ transitions are indicated by the dotted lines. Two optical features clearly anticross on either side of the $X_{\rm hh}$ transition, a clear demonstration of strong coupling.

Figure 3(a) shows the resonant transmission spectrum for the same detuning as figure 2. At this point on the dispersion curve, $k_\parallel = 6.48 \times 10^5$ m^{-1} (2.8°), the composite states are in resonance at 2.616 eV. Two transmission peaks are clearly resolved. Following the standard nomenclature [17], the lower energy peak corresponds to the lower polariton (LP) and the higher energy peak corresponds to the upper polariton (UP). Fitting Lorentzian curves to the LP and UP enables us to determine the peak energy values of the LP and UP. The energies are presented in figure 3(b) (open circles) as a function of $k_\parallel$. Treating the composite states of the polariton as coupled oscillators, the eigenvalues of the coupling Hamiltonian were used to calculate the energy dispersion of the LP and UP taking the Rabi splitting, $\hbar\Omega$, as a fit parameter [18]. The coupled and bare states are displayed as dotted and dashed lines respectively and give good agreement with the experimental data. The point of resonance is found to occur at $\pm 2.8^\circ$ with $\hbar\Omega = 23.6$ meV. The heavy-hole exciton oscillator strength per QW, $f_{X_{\rm hh}}$, can be determined from the Rabi splitting

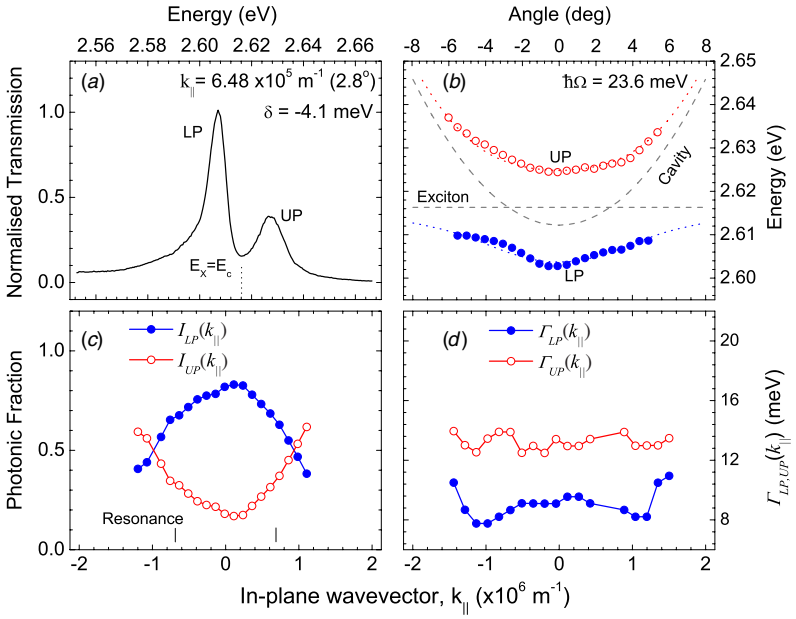

Figure 3. (a) Transmission spectrum on resonance for $\delta = -4.1$ meV and $k_\parallel = 6.48 \times 10^5$ m^{-1} (2.8°). (b) Energy peak values from figure 2 (open circles). Resonance occurs at $k_\parallel = \pm 6.48 \times 10^5$ m^{-1} ($\pm 2.8^\circ$) with $\hbar\Omega = 23.6$ meV. The polariton dispersion curves are compared to the model discussed in the text (dotted lines). Bare cavity and $X_{\rm hh}$ dispersion curves are also shown (dashed lines). (c) Integrated transmission intensity for the lower and upper polariton states. (d) Measured polariton linewidths, $\Gamma_{\rm LP,UP}(k_\parallel)$.

[18], $f_{X_{\rm hh}} = (\hbar\Omega)^2 n_c^2 L_e \epsilon_o m_o / 2e^2\hbar^2 N_{qw}$, where the number of QWs, $N_{\rm qw}$, the cavity refractive index, n_c, and effective cavity length, L_e, are 5, 2.78 and 571 nm respectively. m_o is the free electron mass. For our microcavity we deduce an oscillator strength per QW, $f_{X_{\rm hh}} = 1.78 \times 10^{13}$ cm^{-2}. This is similar to $f_{X_{\rm hh}} \sim 1 \times 10^{13}$ cm^{-2} for MCs studied by Kelkar *et al* [10], but much smaller than the surprisingly high value, $f_{X_{\rm hh}} \sim 7 \times 10^{13}$ cm^{-2}, reported by Pawlis *et al* [11].

The polariton state transmission amplitude is a measure of the polariton composite ratio [19]. In figure 3(*c*) we present the normalized integrated intensities, $I_{\rm LP,UP}(k_\parallel)$, of the LP and UP branches giving a proportional indication of the evolution of the photonic fraction of the polariton. We have defined $I_{\rm LP,UP}(k_\parallel) = I_{lp,up}(k_\parallel)/(I_{\rm lp}(k_\parallel) + I_{\rm up}(k_\parallel))$ such that $I_{\rm LP}(k_\parallel) + I_{\rm UP}(k_\parallel) = 1$. In the angular range of $-4^\circ \leqslant 0 \leqslant +4^\circ$ the LP is predominantly photon-like, indicated by the increase in the LP intensity. Beyond this range, the LP weakens as it becomes progressively more excitonic and $E_{\rm LP}(k_\parallel) \rightarrow E_{X_{\rm hh}}$. The UP behaves inversely. We also note that on resonance, figure 3(*a*), $I_{\rm lp}(k_\parallel) = 2.6 \times I_{\rm up}(k_\parallel)$. $I_{\rm lp}(k_\parallel) = I_{\rm lp}(k_\parallel)$ holds at larger $k_\parallel$ beyond resonance. This is also the case in the MC studied by Kelkar *et al* [10]. The measured linewidths, $\Gamma_{\rm LP,UP}(k_\parallel)$, of the LP and UP are presented in figure 3(*d*). Narrowing of the LP linewidth is clearly evident and occurs at $\sim k_\parallel = \pm 1 \times 10^6$ m^{-1} ($\sim \pm 3^\circ$) [20]. This is evident that the extended nature of the polariton averages out some of the inhomogeneous broadening in the QW exciton.

4. Conclusion

In conclusion, we present a new hybrid technology [15] for fabricating high quality semiconductor microcavities. We have successfully demonstrated three key features of the strong coupling regime: anticrossing of the cavity polariton with a normal mode splitting of 23.6 meV, composite fractional evolution of the LP and UP, and narrowing of the LP linewidth near resonance. We also deduce the heavy-hole exciton oscillator strength per QW to be $f_{X_{\rm hh}} = 1.78 \times 10^{13}$ cm^{-2} for a 8 nm $Zn_{0.9}Cd_{0.1}Se$ QW. Our fabrication technique has eliminated the need for complicated growth-etch-growth processing whilst still employing the advantages of large exciton binding energies found in wide bandgap II–VI materials and high reflectivity offered by dielectric mirrors. Additionally, the epitaxial liftoff technology can potentially be developed to fabricate MCs with MgS/ZnSe quantum wells with an even higher exciton binding energy, ~40 meV [21]. The combination of prolonged photonic lifetimes, due to the achievable high finesse, and the large excitonic oscillator strength are ideally suited to nonlinear phenomena such as parametric scattering and BEC.

Acknowledgment

This work was funded by EPSRC, UK.

References

[1] Weisbuch C, Nishioka M, Ishikawa A and Arakawa Y 1992 Observation of the coupled exciton-photon mode splitting in a semiconductor quantum microcavity *Phys. Rev. Lett.* **69** 3314

[2] Imamoğlu A, Ram R J, Pau S and Yamamoto Y 1996 Nonequilibrium condensates and lasers without inversion: exciton-polariton lasers *Phys. Rev.* A **53** 4250

[3] Dang L S, Heger D, André R, Bœuf F and Romestain R 1998 Stimulation of polariton photoluminescence in semiconductor microcavity *Phys. Rev. Lett.* **81** 3920

[4] Malpuech G, Carlo A D, Kavokin A, Baumberg J J, Zamfirescu M and Lugli P 2002 Room-temperature polariton lasers based on GaN microcavities *Appl. Phys. Lett.* **81** 412

[5] Savvidis P G, Baumberg J J, Stevenson R M, Skolnick M S, Whittaker D M and Roberts J S 2000 Angle-resonant stimulated polariton amplifier *Phys. Rev. Lett.* **84** 1547

[6] Saba M *et al* 2001 High-temperature ultrafast polariton parametric amplification in semiconductor microcavities *Nature* **414** 731

[7] Kasprzak J *et al* 2006 Bose-Einstein condensation of exciton polaritons *Nature* **443** 409

[8] Houdré R, Weisbuch C, Stanley R P, Oesterle U, Pellandini P and Ilegems M 1994 Measurement of cavity-polariton dispersion curve from angle-resolved photoluminescence experiments *Phys. Rev. Lett.* **73** 2043

[9] Madelung O (ed) 1996 *Semiconductors—Basic Data* 2nd edn (Berlin: Springer)

[10] Kelkar P, Kozlov V, Jeon H, Nurmikko A V, Chu C C, Grillo D C, Han J, Hua C Gg and Gunshor R L 1995 Excitons in a II-VI semiconductor microcavity in the strong-coupling regime *Phys. Rev.* B **52** R5491

[11] Pawlis A, Khartchenko A, Husberg O, As D J, Lischka K and Schikora D 2002 Large room temperature Rabi-splitting in a ZnSe/(Zn,Cd)Se semiconductor microcavity structure *Solid State Commun.* **123** 235

[12] Feltin E, Christmann G, Butté R, Carlin J, Mosca M and Grandjean N 2006 Room temperature polariton luminescence from a GaN/AlGaN quantum well microcavity *Appl. Phys. Lett.* **89** 071107

[13] Lohmeyer H, Sebald K, Kruse C, Kröger R, Gutowski J, Hommel D, Wiersig J, Baer N and Jahnke F 2006 Confined optical modes in monolithic II-VI pillar microcavities *Appl. Phys. Lett.* **88** 51101

[14] Robin I C, André R, Balocchi A, Carayon S, Moehl S, Gérard J M and Ferlazzo L 2005 Purcell effect for CdSe/ZnSe quantum dots placed into hybrid micropillars *Appl. Phys. Lett.* **87** 233114

[15] Balocchi A, Curran A, Graham T C M, Bradford C, Prior K A and Warburton R J 2005 Epitaxial lift-off of ZnSe-based heterostructures using a II–VI release layer *Appl. Phys. Lett.* **86** 011916

[16] Bradford C, O'Donnell C B, Urbaszek B, Balocchi A, Morhain C, Prior K A and Cavenett B C 2001 Growth of zinc blende MgS and MgS/ZnSe quantum wells by MBE using ZnS as a sulphur source *J. Cryst. Growth* **227** 634

[17] Kavokin A and Malpuech G 2003 *Cavity Polaritons* (Amsterdam: Elsevier)

[18] Savona V, Andreani L C, Schwendimann P and Quattropani A 1995 Quantum well excitons in semiconductor microcavities: unified treatment of weak and strong coupling regimes *Solid State Commun.* **93** 733

[19] Hopfield J J 1958 Theory of the contribution of excitons to the complex dielectric constant of crystals *Phys. Rev.* **112** 1555

[20] Kavokin A V 1998 Motional narrowing of inhomogeneously broadened excitons in a semiconductor microcavity: semiclassical treatment *Phys. Rev.* B **57** 3757

[21] Urbaszek B, Balocchi A, Bradford C, Morhain C, O'Donnell C B, Prior K A and Cavenett B C 2000 Excitonic properties of MgS/ZnSe quantum wells *Appl. Phys. Lett.* **77** 3755